CHARM facility remotely controlled platform at CERN: A new fault-tolerant redundant architecture

CHARM Facility Remotely Controlled Platform at CERN: a New Fault-Tolerant Redundant Architecture

A. Toscani[a], D. Santoro[a], N. Delmonte[a], P. Cova[a], C. Concari[a], A. Lanza[b,*]

[a] *Department of Engineering and Architecture, University of Parma, Parco Area delle Scienze 181/a, 43124, Parma, Italy*

[b] *INFN Pavia, via Agostino Bassi, 6, 27100 Pavia, Italy*

Abstract

Many power electronics applications require high tolerance to faults such as short circuit or open circuit of the control signals. One such application is the CERN High energy AcceleRator Mixed-field (CHARM) facility, where maintenance may be precluded for long periods of time due to radiation and, therefore, high reliability is necessary. A redundant interconnection architecture for the control signals is proposed, where each signal is individually processed by different CPUs and transmitted through separate interconnection lines. During normal operation, the CPUs are synchronized and produce the same signals. The purpose of the proposed hardware and firmware strategy is to allow the actuator to continue operating even in case of fault; regardless of the fault type (open circuit, short circuit to ground or to positive supply), a fault on one of the parallel lines would not inhibit the correct operation of the remaining line.

This solution can be used to control the movements of a target system using a remote joystick in a safe environment. The architecture features reliable transmission of PWM signals driving a half-bridge power converter. Moreover, it is possible to extend it to any type of converter such as three-phase bridges, three-level NPC, or buck-boost converters.

Simulations and experimental results show a good agreement, proving the effectiveness of the proposed fault-tolerant circuitry.

1. Introduction

Power electronic systems are used in countless applications and environments. The requirements can be very different, and the system reliability can assume varying degrees of importance. Very highly fault-tolerant architectures are required in safety critical applications. Depending on the type of hardware redundancy used, many fault-tolerant techniques for power electronic converters can be implemented [1]. The power stage topology can be designed to allow many additional improvements at the system level and to achieve highly reliable operation continuity [2]. Another consideration can be done on the type of error that occurs most often and needs to be handled. If we consider a general electronic application, soft errors should be considered as of critical impact for the systems [3], thus, in power electronic applications, short circuits to the ground or to the power supply rail, as well as open circuits, can be considered as the most critical faults. Numerous detection techniques and fault-tolerant system architectures can be found in literature for power electronic applications. In [4], a method for modular multilevel converters fault diagnosis and tolerant control is proposed. In this case, redundant IGBT submodules are activated when one of the typical faults is detected, and a tolerant control of the PWMs ensures the operation continuity. Still for multilevel converters, different methods are proposed in [5,6]. In these cases, the redundant switching states are used instead of increasing the submodules, and the fault control consists in turning off the corresponding leg control switch, reducing the power transfer capability. In the applications of multilevel converters with batteries, the converter control can also be designed for fault tolerance to storage failures [7]. In [8], isolated full-bridge DC-DC converter topologies are taken into consideration. An auxiliary winding was added to the transformer, on which the diagnosis occurs. In case of faults, the system power capability decreases, and it works through an asymmetrical half-bridge. Tradeoffs can be reached depending on the application. In the case of photovoltaic DC-DC converter failures, it's possible to add a few components and apply control methods to maintain power transfer to battery or to load without turning off the whole system [9], or adding a strategical redundant power switch for power transfer continuity [10]. Also for AC motor drive systems, many solutions can be found in terms of fault tolerant topologies and redundancy trade-off [11], or by adding specific TRIAC switches for a converter topology reconfiguration [12]. As shown in [13], fault-tolerance techniques for multilevel inverters require an approach based on both hardware and software reconfigurations. On the other hand, for two-level inverters, it is more common to focus on hardware redundancy and reconfiguration. The main common element of fault-tolerant systems can be identified in the redundancy of targeted system hardware, mostly with modularly added devices and interconnections, allowing to maintain partial

* Corresponding author. agostino.lanza@pv.infn.it
Tel: +39 0382 987324; Fax: +39 0382 423241

operation continuity through the reduction of power transfer capability [14,15].

Fail-safe systems like the ones cited above, help prevent simple faults from developing into failures at system level, but could become very expensive solutions to [16]. This paper presents a redundant circuit to boost the availability of the power stage control without the need to detect the fault type. Usually, in literature, redundancy is obtained using magnetic coupling (i.e. transformers) [8]: the redundant signals supply different primary windings of a transformer and the output signal is taken from the secondary winding. In our application, magnetic coupling is not applicable because of the potential presence of high magnetic fields that can cause saturation of the transformer core. The proposed solution, instead, uses capacitive coupling, in order to avoid this kind of problem. In environments such as at the CERN CHARM facility, maintenance can be precluded for long periods, due to high radiation levels during and after experiments. Therefore, availability and fault-tolerance should be assured with any type of fault on the control stage.

In this work, the redundancy is obtained starting from the Micro Processor Units (MPUs), which are redundant and synchronized in normal operation mode, but autonomous if one of them fails. Regardless of the fault type (open circuit, short circuit to ground or to positive supply), a fault on one of the parallel lines does not inhibit the correct operation of the remaining line. The transmission is redundant and modular as shown in Fig. 1, considering one line per MPU, and only at the final stage, before the power converter, a simple coupling circuit is able to select only good control signals.

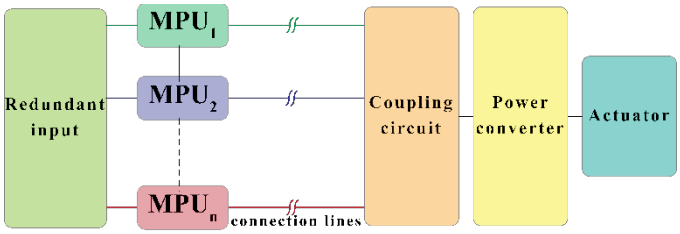

Fig. 1 – Modular proposed architecture of the control platform.

The second section of this paper introduces the CERN CHARM facility, where the high reliability requirements are motivated. Then, the operating principle of the proposed solution is explained. Section 4 shows the simulation and experimental results, with different fault tests.

2. The application: CERN CHARM facility

The CERN High energy AcceleRator Mixed-field (CHARM) [17] is an infrastructure of the Centre Europeén pour la Recherche Nucléaire (CERN) near Geneva (Switzerland), able to generate a radiation background as much as possible similar to the one created by the CERN main accelerator, the Large Hadron Collider (LHC), in order to test electronics components, devices, and detectors. This radiation field can be made similar to other environments like Ground, Atmospheric and Space conditions for allowing specific system tests [18,19].

The layout of the facility is represented in Fig. 2. The primary particle source is the Proto Synchrotron (PS) accelerator proton beam at an energy of 24 GeV/c (the blue line in Fig. 2), impinging on a target system made of two different materials (copper and aluminum) in three combinations (bulky copper, bulky aluminum and aluminum with holes). The target system, visible in Fig. 3, is installed on a remotely controlled platform, which is movable in or out of the beam line (see Fig. 2 for its position), and can select which of the three target types to position on beam by a remote command. All movements are implemented by using actuators like stepper motors or DC motors.

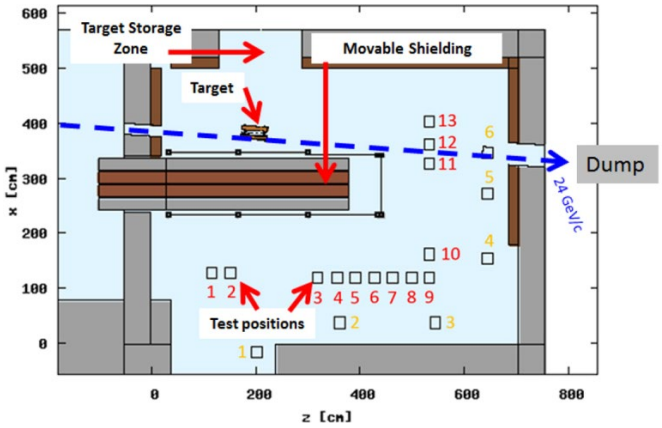

Fig. 2 – Layout of the CHARM facility.

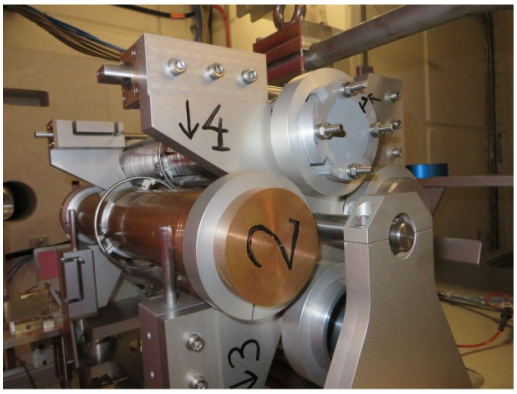

Fig. 3 – The CHARM target system.

The device under test (DUT), one or more, is installed on a mini-rack, which is placed in one of the several positions marked in red and yellow in Fig. 2, depending on the required radiation dose and fluence. The mini-rack is equipped with the DUTs in the safe zone, and moved in one of the allowed positions by means of an automated conveyor system from the company AVT Europe NV, shown in Fig. 4. All cables and cooling/gas pipes are collected in large flexible chains running on a rail system on the ceiling, so they can follow the conveyor up to the selected position with a very reduced

friction and weight. One such chain is visible in Fig. 4, connected to the conveyor.

In order to get a high radiation gradient in the relatively small area of the facility, a movable shielding system between the test area and the target has been implemented. Its position is depicted in Fig. 2. It is composed of four plates, two made of concrete and the other two of iron. Each one can be inserted or removed from the support cage, so the several possible combinations of their positions realize different radiation field intensities. Their movement is remotely controlled.

Fig. 4 – The automated conveyor chariot.

All these three systems, the target positioning and selection, the placement of the DUT on the selected position and the position of the shielding plates for field attenuation, cannot be managed manually, and in case of malfunctioning or damage cannot be accessed or visually inspected with webcams by humans, even after weeks of beam off, due to the activation of the metallic structure. For this reason, the control of the electro-mechanical actuators must have the maximal reliability under any operating condition.

3. The proposed solution

As an example, the remote control of the target platform is taken into consideration, describing in the following a circuit able to cope with the facility requirements in terms of reliability.

The control system uses a 20 kHz PWM signal, where the duty cycle determines the movement speed of the controlled platform. The redundant circuit uses the PWM signal to on-off keying (OOK) modulate a 2-MHz square-wave signal with the required PWM control signal similarly to [20]. The signal is transmitted in the CHARM facility, decoupled near the power stage, and filtered to achieve the original PWM signal.

The flow chart of the used algorithm is shown in Fig. 5. For each period of the 20 kHz PWM, the ADC channel for the joystick sensing is checked, and both MPUs generate OOK modulated 2 MHz signals. During the period, the MPUs sense the 20 kHz PWM for the synchronization.

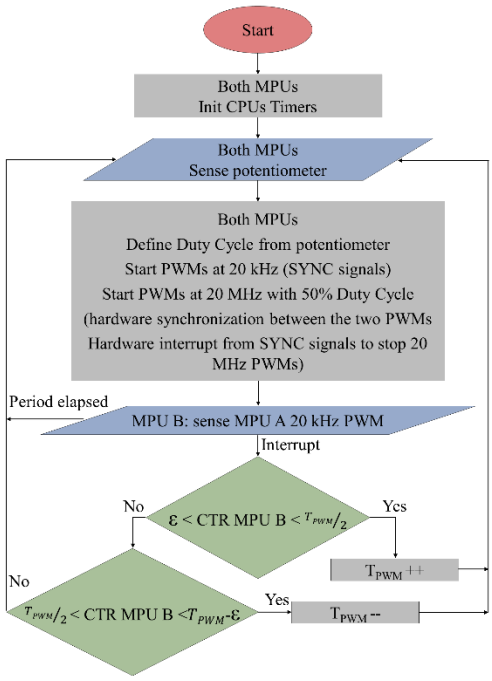

Fig. 5 – Flow chart of the implemented algorithm.

The proposed architecture where the algorithm is applied to two CPUs is shown in Fig. 6.

To increase the availability of the architecture, the CPUs are supplied by different power converters, and the joystick has redundant outputs as in Fig. 7. Each axis (X and Y) drives two different potentiometers that are read by an MPU. In this way, MPU1 reads the voltage divider outputs X1 and Y1, while MPU2 reads the outputs X2 and Y2. The potentiometers read by MPU1 are supplied using a different DC/DC converter than those read by MPU2. Each MPU samples the input signal of the potentiometer, and the value of this signal is used to determine the ON time and the OFF time of the PWM output at 20 kHz (Fig. 8).

This signal is then used to modulate a high frequency square signal, so that during the ON time the transmitted signals are 2 MHz (f_{HF}) square waves. All the MPUs generate the same signals, and all of them are routed to a unique output using a "wired-or" operation realized by means of two diodes. The output is then low-pass filtered and squared by a Schmitt trigger to obtain the original information.

To correctly design the circuit and determine the components sizing, we have to consider the different working regions. In fact, when the high frequency signal has to be coupled and, at the same time, fault signals have to be decoupled, the capacitor C_{IN} plays the key role. For this purpose, magnetic components have not been used in order to avoid core saturation problems due to the possible presence of high magnetic fields.

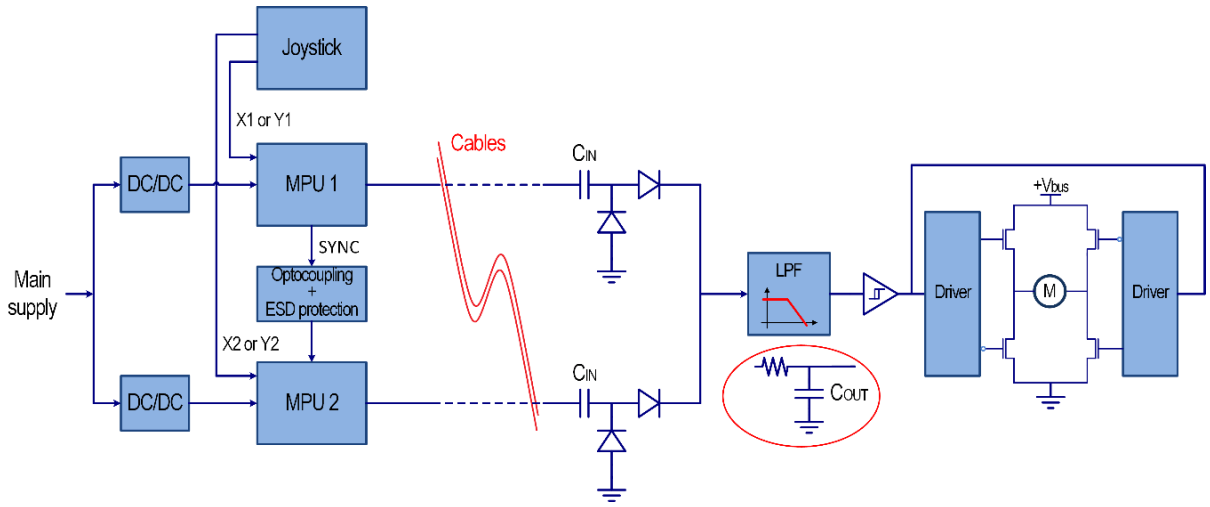

Fig. 6 – Proposed architecture.

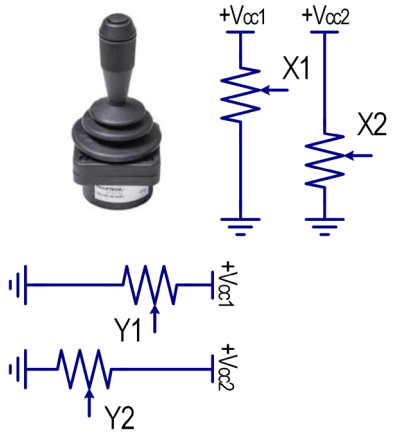

Fig. 7 – The redundant joystick.

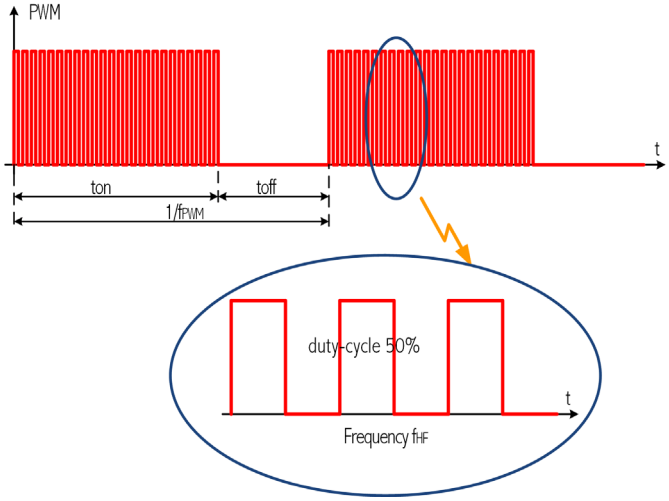

Fig. 8 – Output signal specification.

In this work, with a 2 MHz signal frequency, a 3.3 nF capacitor has been used. This allows to couple the working frequency and to have good high output voltage peaks. In fact, as a high pass filter, the coupling capacitor should be higher than $\frac{1}{2\pi f_c R_i}$, where the frequency f_c can be chosen considering the attenuation introduced by the filter $\frac{1}{\sqrt{1+(f_c/f)^2}}$. In our case, a f_c of about 15 kHz has been chosen.

Different considerations must be made on the filter capacitor C_{OUT}. In this case, it should be smaller than the coupling capacitor in order to discharge in a reasonable time and avoid unacceptable signal delays. At the same time, the ripple must be limited, and higher capacitor values allow a smaller output signal ripple. In this work, a 330 pF capacitor has been used, with a 3.3 kΩ output resistor in parallel. Here, the cutting frequency must be higher than the one chosen for the coupling capacitor, and the difference between the two determines a precise bandwidth. In our case, the f_t chosen for the low pass filter is about 150 kHz. This is a little less than $f_{HF}/10$.

The PWM synchronization between the MPUs is a very important task. A good synchronization of the timers that generate the PWM signals is required for correct operation; even a small tolerance of 5–10 ppm of different crystals of the MPUs can lead to a phase difference that needs to be compensated.

An algorithm was developed and implemented in software for this task [21,22]. The first MPU generates a pulse (SYNC signal) in correspondence with the reload of the timer that generates its PWM; this signal is received by other MPU(s) of the chain, and every slave MPU in this way can measure the delay between its PWM reload and the reload of the previous MPU of the chain. The measured delay is used to correct the phase shift of different PWMs.

A dedicated algorithm makes the needed adjustments to synchronize all the PWM frequencies. The measured displacement range is from zero to the modulus of the PWM carrier.

The fixing action needed to synchronize the PWM pulses of the MPUs depends on the displacement value: if the displacement is from zero to a half period of the PWM carrier, the algorithm anticipates the MPU PWM reload (by a

temporary decrease of its PWM period, Fig. 9-a); vice versa, if the displacement is larger than a half period of the PWM carrier, the algorithm delays the MPU PWM reload (by a temporary increase of its PWM period, Fig. 9-b). If the displacement is below a certain threshold (a very small part of the PWM period) no corrective action is needed. The described algorithm is depicted in Fig. 10.

This is the fastest way to perform the synchronization (Fig. 11). When the displacement is greater than the period of the PWM carrier, it means that there is a loss in the synchronization signal and a watchdog disables the PWM signal of the involved MPU, while the SYNC signal bypasses the MPU.

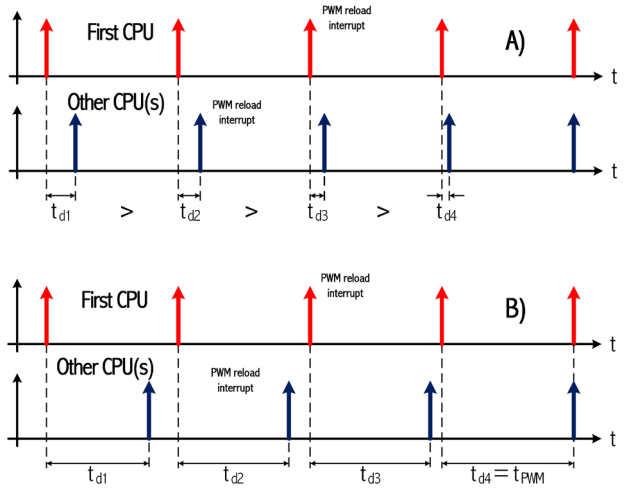

Fig. 9 – The temporal evolution of the effects of the synchronization algorithm on the PWM reloads. Case A) – anticipating MPU PWM reload; case B) – delaying MPU PWM reload).

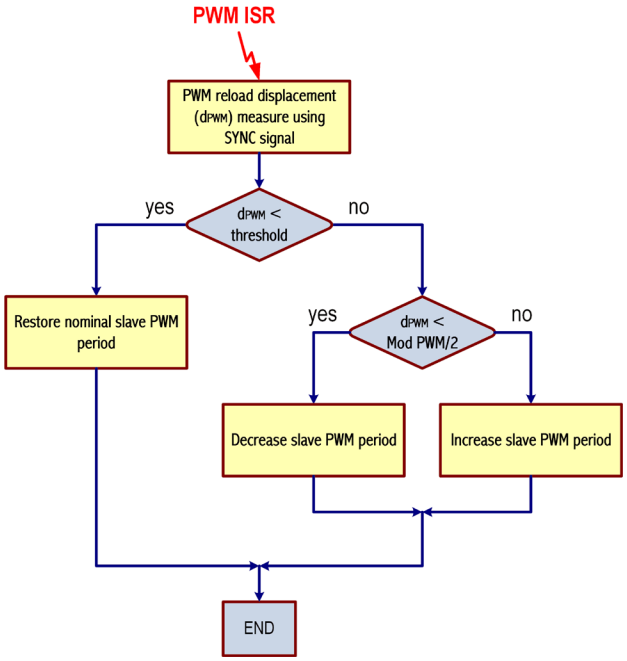

Fig. 10 – PWM synchronization algorithm.

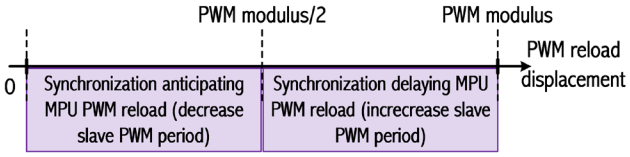

Fig. 11 – PWM synchronization strategy.

4. Simulation and experimental tests

The proposed architecture has been simulated using MATLAB/Simulink. Different kind of hard faults have been simulated: open circuit, short circuit to ground, and short circuit to the power rail.

Fig. 12 shows the simulation results of the architecture without faults (normal operation). The two high frequency modulated signals are the black and red ones. The blue signal represents signal 1 after the decoupling capacitor, but before the Schottky diode and the connection with signal 2. The green waveform represents the output signal, where the signals 1 and 2 are coupled and the low-pass filter envelopes the original PWM signal.

The short circuit fault to the positive power rail has been simulated adding a controlled switch, which connects signal 1 to the power supply. For a better comparison with the experimental tests, the faults were simulated starting from a fault condition and then moving to normal operating condition. Fig. 13 shows the short circuit to power rail. In black and red the two modulated signals, in blue the signal 1 after the decoupling capacitor, while the green curve represents the output signal.

The same simulation model has been used for the short circuit of the signal 1 to ground. In Fig. 14, the black and red waves represent the two modulated signals, in blue the signal 1 after the decoupling capacitor, and the green curve represents the output signal.

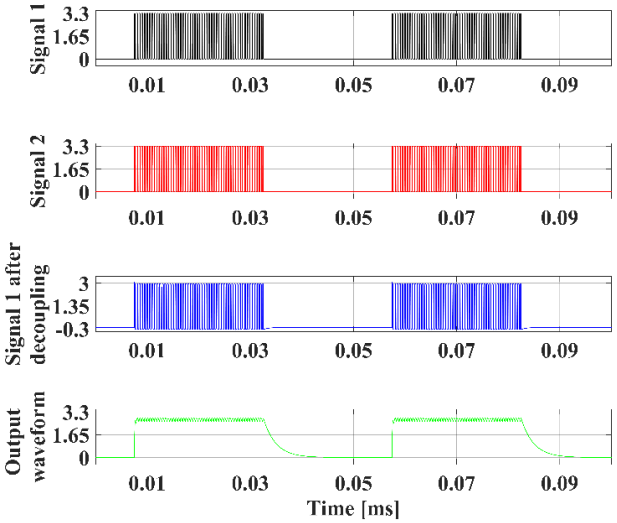

Fig. 12 – Simulation results without faults (normal operation).

Finally, a last simulation was carried out for the cable disconnected fault. As for the other cases, changes cannot be detected on the output voltage, thus, the voltage on the

disconnected sides' coupling circuit needs one on-keying cycle to be discharged. Fig. 15 shows the simulation results, with the same colour coding of the other simulations.

To validate the simulation results, a prototype circuit has been developed. Firstly, short connections between the MPU outputs and coupling circuit have been used for a circuit verification and clean output results. Fig. 16 shows the experimental results in normal operating mode. The original PWM signal at 20 kHz is the blue one. The red signal is the modulated signal at high frequency (2 MHz). The green trace represents the output signal, where the signals are coupled and the low-pass filter yields the original PWM signal. The magenta trace represents the output squared by the Schmitt trigger.

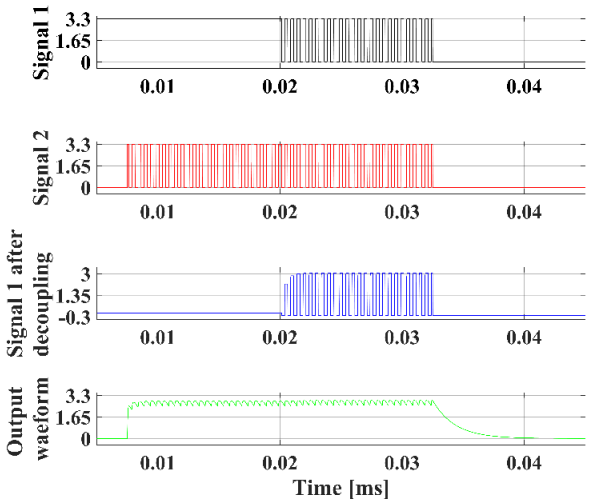

Fig. 13 – Simulation results with signal 1 short-circuited to the power rail.

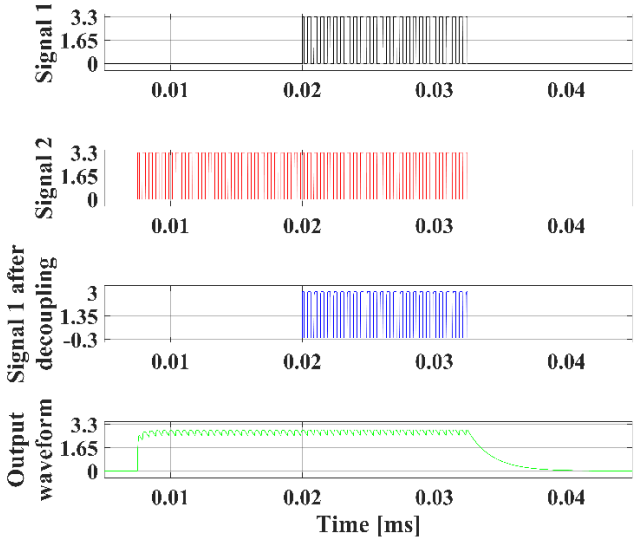

Fig. 14 – Simulation results with signal 1 short-circuited to ground.

With the same operating conditions, without faults, the circuit has been tested with long cable connections: approximately 10 m, as required by the application. Fig. 17 shows the experimental results.

Finally, the experimental tests have been repeated with fault conditions. One of the two signals has been connected during the operating cycle keeping the trigger on 1.65 V and setting the oscilloscope to single capture mode. Fig. 18 shows the experimental results with a short circuit to power supply. As in the simulations, also the short circuit to ground fault has been tested. Fig. 19 shows the experimental results with same signal colour identification as the previous experiment.

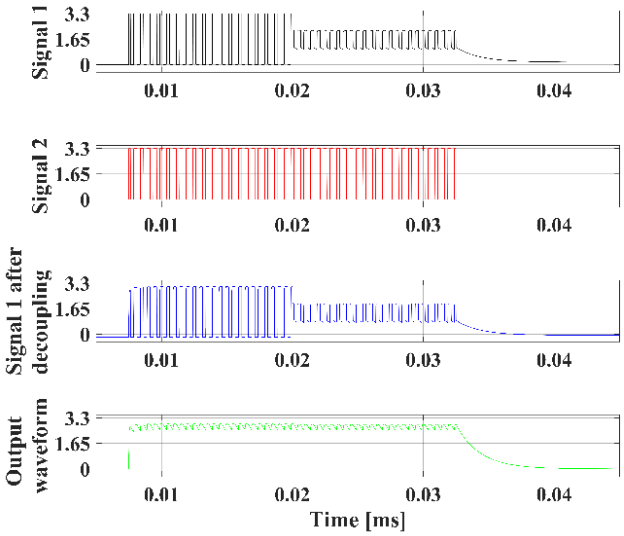

Fig. 15 – Simulation results with signal 1 disconnected.

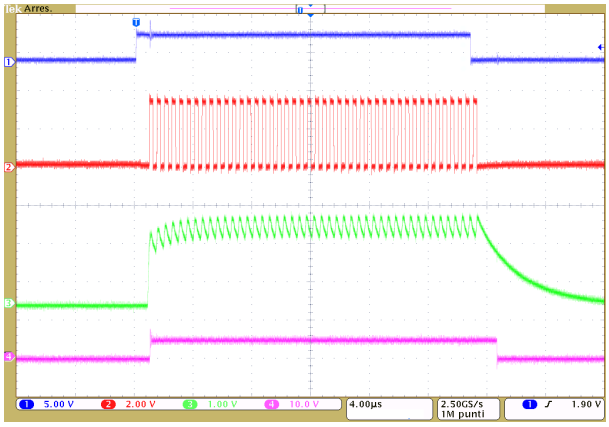

Fig. 16 – Experimental results without faults.

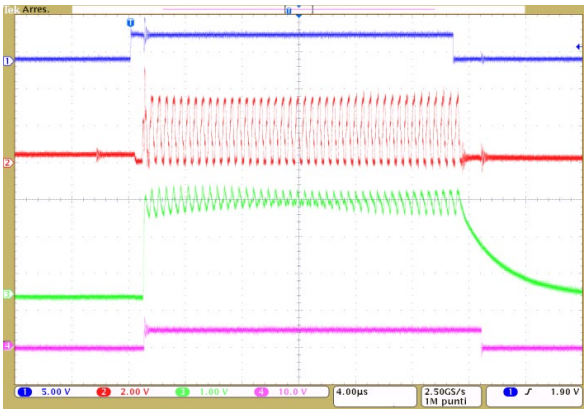

Fig. 17 – Experimental results with long cable (10 m) connections, no faults.

In addition, the disconnected cable fault condition has been tested, but considering that in the experimental the starting condition is fault, and the signals are triggered when operating in normal mode, results are similar to those shown in Fig. 19, and therefore not shown again. To provide complete experimental tests, Figs 20, 21 and 22 represent the experimental results with a sinusoidal input signal, with and without fault condition. In these cases, the joystick has been bypassed and the PMW duty cycle of the modulating signal changes continuously, following the sinusoidal input.

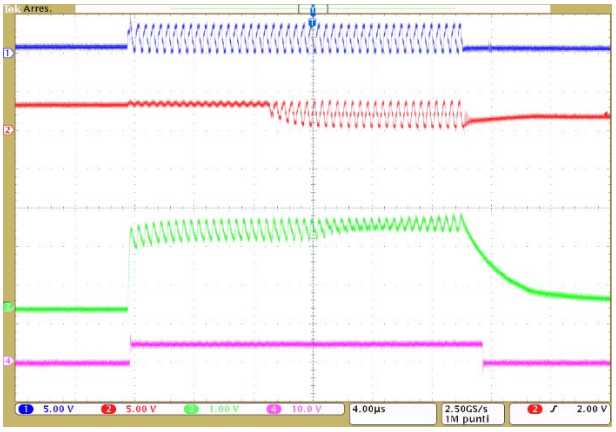

Fig. 18 – Experimental results with signal 1 short-circuited to the positive power rail.

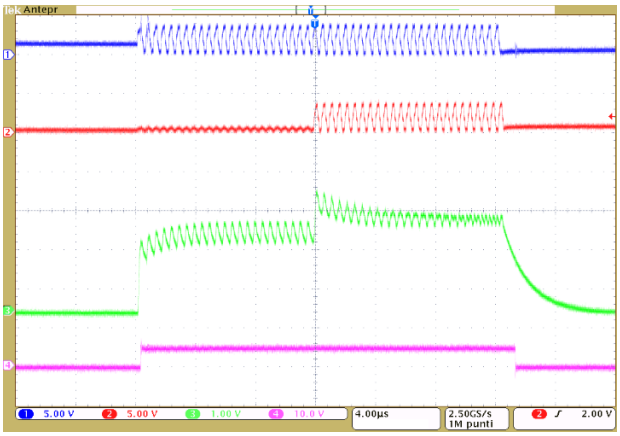

Fig. 19 – Experimental results with signal 1 short-circuited to ground.

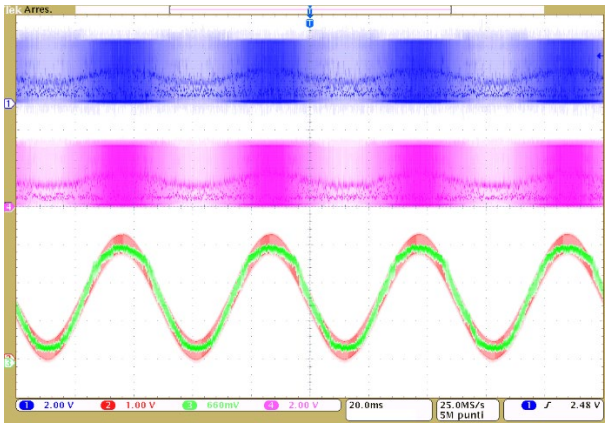

Fig. 20 – Experimental results with sinusoidal input reference in normal operating mode.

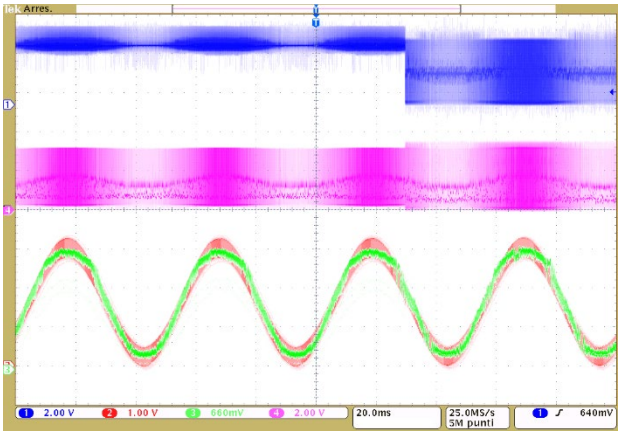

Fig. 21 – Experimental results with sinusoidal input reference and fault condition: short circuit of signal 1 to the positive power rail.

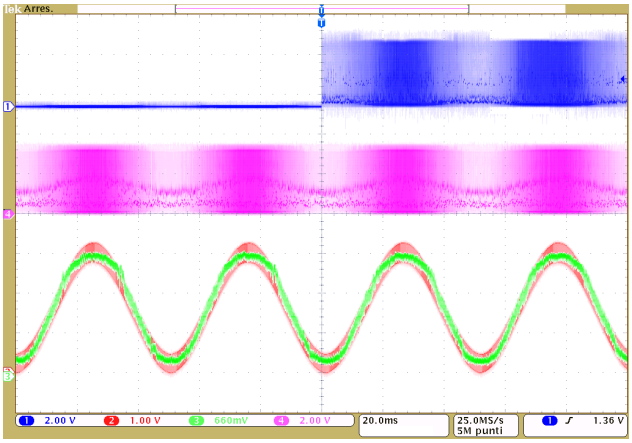

Fig. 22 – Experimental results with sinusoidal input reference and fault condition: short circuit of signal 1 to ground.

5. Discussion and conclusions

This paper proposes a new fault tolerant control architecture in which redundant control signals are individually generated by different CPUs and transmitted through separate interconnection lines. This solution is specifically designed for the remote-controlled platform of the CERN High energy AcceleRator Mixed-field (CHARM) infrastructure, where maintenance may not be possible for extended periods, and high reliability is necessary. The platform uses two motors for x and y axes motion, each driven by one of the proposed redundant circuits. In order to avoid the risk of core saturation due to the possible presence of high magnetic fields, the adopted hardware does not use magnetic components.

The proposed solution was simulated using the MATLAB/Simulink environment, and a prototype was built and fully tested. Tests and simulations include various types of faults (short circuit to ground, short circuit to the positive power rail, cable disconnected) showing the highest grade of fault tolerance and reliability.

In order to quantify the system reliability improvement in term of time to failure or failure rate, one should know the

reliability parameters, and then the failure mechanisms, for any part of the system, from devices, to boards, and cables. These parameters are strictly dependent on the environmental conditions and are, a priori, unknown. The reliability improvement of the proposed architecture is related to the introduced redundancy, which includes the transmission path from the control unit to the electric drive. Generally, a 1+n redundancy of the whole transmission chain can be implemented, and then its reliability can be highly improved, but a quantitative result cannot be calculated, since in this case there isn't a statistical fault history to base estimates on.

Additional cost of the system is practically negligible in the proposed application, where a stop imposed by a fault would have orders of magnitude higher costs. The only possible drawback of the presented system can be related to the additional room needed for doubling cables, but this is not a considerable issue in the proposed application. Indeed, the proposed system requires an additional PCB with a size of a few cm^2 to make a circuit with a negligible volume with respect to the one needed for the additional cabling. Moreover, power consumption of the additional board is negligible in the whole power system, and it is not a concern.

Although the proposed architecture has been designed for a full-bridge power converter, it is possible to apply it to any type of PWM-based converter, such as three-phase bridge, three-level NPC, or buck-boost converters.

References

[1] W. Zhang, D. Xu, P.N. Enjeti, H. Li, J.T. Hawke, H.S. Krishnamoorthy, Survey on fault-tolerant techniques for power electronic converters, IEEE Trans. Power Electron. 29 (2014) 6319–6331. https://doi.org/10.1109/TPEL.2014.2304561.

[2] U.M. Choi, F. Blaabjerg, K.B. Lee, Reliability improvement of a T-type three-level inverter with fault-tolerant control strategy, IEEE Trans. Power Electron. 30 (2015) 2660–2673. https://doi.org/10.1109/TPEL.2014.2325891.

[3] N. Eftaxiopoulos, N. Axelos, K. Pekmestzi, DIRT latch: A novel low cost double node upset tolerant latch, Microelectron. Reliab. 68 (2017) 57–68. https://doi.org/10.1016/j.microrel.2016.11.006.

[4] B. Li, S. Shi, B. Wang, G. Wang, W. Wang, D. Xu, Fault diagnosis and tolerant control of single IGBT open-circuit failure in modular multilevel converters, IEEE Trans. Power Electron. 31 (2016) 3165–3176. https://doi.org/10.1109/TPEL.2015.2454534.

[5] S. Tang, X. Yin, D. Wang, C. Zhang, Z. Shuai, X. Yang, Z.J. Shen, J. Wang, Detection and identification of power switch failures for fault-tolerant operation of flying capacitor Buck-boost converters, Microelectron. Reliab. 88–90 (2018) 1246–1241. https://doi.org/10.1016/j.microrel.2018.06.102.

[6] G. Yang, C. Fu, H. Yi, C. Chai, B. Huang, S. Hao, Z. Chen, Direct power control of three-level NPC grid-connected system combined with fault-tolerant technology, Microelectron. Reliab. 88–90 (2018) 1057–1062. https://doi.org/10.1016/j.microrel.2018.07.140.

[7] Y.X. Zhao Liu, Shuai Wang, Zhendong Ji, Xiaopeng Ji, A novel fault-tolerant control for battery-energy-storage system based on cascaded multilevel converter with battery/BMS failure, Microelectron. Reliab. 88–90 (2018) 1268–1273.

[8] X. Pei, S. Nie, Y. Chen, Y. Kang, Open-circuit fault diagnosis and fault-tolerant strategies for full-bridge dc-dc converters, IEEE Trans. Power Electron. 27 (2012) 2550–2565. https://doi.org/10.1109/TPEL.2011.2173589.

[9] E. Ribeiro, A.J.M. Cardoso, C. Boccaletti, Fault-tolerant strategy for a photovoltaic DC-DC converter, IEEE Trans. Power Electron. 28 (2013) 3008–3018. https://doi.org/10.1109/TPEL.2012.2226059.

[10] D. Oulad-Abbou, S. Doubabi, A. Rachid, Power switch failures tolerance of a photovoltaic fed three-level boost DC-DC converter, Microelectron. Reliab. 92 (2019) 87–95. https://doi.org/10.1016/j.microrel.2018.11.017.

[11] B.A. Welchko, T.A. Lipo, T.M. Jahns, S.E. Schulz, Fault tolerant three-phase AC motor drive topologies; A comparison of features, cost, and limitations, in: IEMDC 2003 - IEEE Int. Electr. Mach. Drives Conf., 2003. https://doi.org/10.1109/IEMDC.2003.1211315.

[12] R.L. De Araujo Ribeiro, C.B. Jacobina, E.R. Cabral da Silva, A.M. Nogueira Lima, Fault-tolerant voltage-fed PWM inverter AC motor drive systems, IEEE Trans. Ind. Electron. 51 (2004) 439–446. https://doi.org/10.1109/TIE.2004.825284.

[13] B. Mirafzal, Survey of fault-tolerance techniques for three-phase voltage source inverters, IEEE Trans. Ind. Electron. 61 (2014) 5192–5202. https://doi.org/10.1109/TIE.2014.2301712.

[14] D. Siemaszko, S. Pittet, Impact of modularity and redundancy in optimising the reliability of power systems that include a large number of power converters, Microelectron. Reliab. 51 (2011) 1484–1488. https://doi.org/10.1016/j.microrel.2011.07.056.

[15] K. Siri, C.Q. Lee, T.E. Wu, Current Distribution Control For Parallel Connected Converters: Part I, IEEE Trans. Aerosp. Electron. Syst. 28 (1992) 829–840. https://doi.org/10.1109/7.256303.

[16] M. Blanke, R. Izadi-Zamanabadi, S.A. Bøgh, C.P. Lunau, Fault-tolerant control systems - A holistic view, Control Eng. Pract. 5 (1997) 693–720. https://doi.org/10.1016/S0967-0661(97)00051-8.

[17] A. Thornton, CHARM Facility test Area Radiation Field Description, Cern. - Intern. Note. (2016).

[18] J. Mekki, M. Brugger, R.G. Alia, A. Thornton, N.C.D.S. Mota, S. Danzeca, CHARM: A Mixed Field Facility at CERN for Radiation Tests in Ground, Atmospheric, Space and Accelerator Representative Environments, IEEE Trans. Nucl. Sci. 63 (2016) 2106–2114. https://doi.org/10.1109/TNS.2016.2528289.

[19] J. Ameel, D. Amidei, S. Baccaro, M. Citterio, P. Cova, N. Delmonte, K. Sekhon Edgar, R. Edgar, S. Fiore, A. Lanza, S. Latorre, M. Lazzaroni, Y. Yang, Radiation-hard power electronics for the ATLAS New Small Wheel, J. Instrum. 10 (2015). https://doi.org/10.1088/1748-0221/10/01/C01009.

[20] F. Troni, C. Concari, A. Toscani, G. Buticchi, G. Franceschini, Fault tolerant PWM generation with doubleredundant logic, in: WIT Trans. Eng. Sci., 2014. https://doi.org/10.2495/AMITP20130581.

[21] P. Cova, A. Toscani, C. Concari, G. Franceschini, M. Portesine, Comprehensive Control System for Parallelable 60 Hz-2MVA Harbor AC/AC Converters, IEEE Trans. Ind. Informatics. 14 (2018) 2432–2441. https://doi.org/10.1109/TII.2017.2776155.

[22] C. Concari, P. Cova, G. Franceschini, A. Toscani, F. Bertoluzza, Improved control strategy for modular 2MVA AC/AC power converter, in: 2013 IEEE Energy Convers. Congr. Expo. ECCE 2013, 2013: pp. 5294–5300. https://doi.org/10.1109/ECCE.2013.6647418.